

# Bioactive coatings prepared by sol–gel on stainless steel 316L

C. García <sup>a</sup>, S. Ceré <sup>b</sup>, A. Durán <sup>c,\*</sup>

<sup>a</sup> Universidad Nacional de Colombia, Sede Medellín, A.A. 3840 Medellín, Colombia

<sup>b</sup> INTEMA-Universidad Nacional de Mar del Plata, Argentina, Juan B. Justo 4302, B7608FDQ Mar del Plata, Argentina

<sup>c</sup> Instituto de Cerámica y Vidrio (CSIC), Campus de Cantoblanco, 28049 Madrid, Spain

## Abstract

This work describes the development and characterization of coatings obtained by the sol–gel technique, applied on stainless steel used in orthopaedic surgery. These coatings are applied to reduce metal corrosion and adverse reactions when implanted. Hybrid coatings of silica containing hydroxyapatite, bioactive glass and glass–ceramic particles were prepared and applied on metal substrates. The coated samples were further tested in vitro to study their electrochemical properties and bioactive response. The electrochemical properties were evaluated by means of potentiodynamic polarization assays using simulated body fluid (SBF) as electrolyte. In vitro bioactivity tests were performed by soaking the coated samples in SBF at 37 °C with a ratio sample area/fluid volume of 0.35 cm<sup>2</sup>/ml for different periods. The coatings improve corrosion resistance of the steel substrate and in vitro tests revealed that all the films show signs of bioactivity.

© 2004 Elsevier B.V. All rights reserved.

PACS: 81.20.Fw; 81.15.–z; 81.65.Kn; 82.80.Fk

## 1. Introduction

Orthopaedic implants are mainly made of metals to endure mechanical stresses in service. Among the most commonly alloys used for orthopaedic implants are titanium alloys, cobalt alloys and stainless steel 316L. Their main characteristic is their mechanical properties but varying in degrees, there is always a concern about their corrosion resistance in physiological fluids and their bioactivity. The need to reduce costs in public health services has compelled the use of stainless steel as the most economical alternative for orthopaedic implants [1]. For this reason, it is important in the development of techniques to improve the corrosion resistance and bioactivity of this material. Coating application by sol–gel technique is a promising alternative due to its properties and tailoring possibilities [2–11].

Different coatings have been applied onto stainless steel for various applications, including biomedical uses [1,4,5,7]. In particular, coatings containing bioactive glass particles have corrosion resistance and bioactivity [6,7].

The aim of this work is to obtain sol–gel coatings containing bioactive glass, glass ceramic and hydroxyapatite particles on stainless steel 316L and evaluate them by means of in vitro tests and electrochemical analysis.

## 2. Experimental procedures

### 2.1. Particle preparation

The bioactive parent glass belongs to the system CaO–SiO<sub>2</sub>–P<sub>2</sub>O<sub>5</sub> with 57.44% CaO, 35.42% SiO<sub>2</sub> and 7.15% P<sub>2</sub>O<sub>5</sub> in molar percentages. It was obtained by melting the oxides at 1600 °C for 2.5 h and posterior quenching in water to room temperature [6,7]. Bioactive glass ceramic particles were obtained from the

\* Corresponding author. Tel.: +34 91 7355840; fax: +34 91 7355843.  
E-mail address: [aduran@icv.csic.es](mailto:aduran@icv.csic.es) (A. Durán).

previously described glass through a heat treatment of 2 h at 1050 °C to induce crystallization of hydroxyapatite and wollastonite. Hydroxyapatite was prepared by precipitation from an aqueous solution of tetra hydrated calcium nitrate and ammonium phosphate, in concentrations 1 M and 0.48 M, respectively, in basic media (pH = 10), followed by a heat treatment of 1050 °C during 1 h [12]. All the bioactive particles were milled in a planetary mill (Fritsch Pulverisette, Germany), with agate jar and balls at 1500 rpm for a maximum period of 7 h. After milling, the powders were sieved and the particle size distribution was measured, using a laser diffraction equipment (Mastersizer S, Malvern, UK). The specific surface area was determined using a N<sub>2</sub>-adsorption BET equipment (Monosorb, Quantachrome, USA).

## 2.2. Sol–gel preparation

Silica sols were prepared by acid catalysis in a single stage. Tetraethylorthosilicate (TEOS, ABCR) and methyltriethoxysilane (MTES, ABCR) were selected as silica precursors for the sol, prepared in alcoholic media and using HNO<sub>3</sub> 0.1 N and acetic acid as catalysts. The molar ratio TEOS:MTES was defined as 40:60, the H<sub>2</sub>O:(TEOS + MTES) ratio was 2:1, and the water: acetic acid ratio was 7:1, to give a final concentration of SiO<sub>2</sub> of 200 g/l.

The suspensions were prepared by adding 10 wt% of particles to the silica sols, stirring them with a high shear mixer (Silverson L2R, UK) during 6 min. The addition of tetrapropyl ammonium hydroxide (TPAH, Aldrich) in a concentration of 50 wt% with respect to solids, was used for maintaining glass and glass ceramic particles in suspension. TPAH acts as a cationic surfactant being adsorbed on the particles; it also increases the pH to 6–7 moving the solution away from the isoelectric point and favoring electrostatic repulsion among the particles [8]. The suspension with hydroxyapatite particles was obtained by adding a phosphate ester (Emphos PS21, Whitco, Chem, USA) 2 wt% with respect to solids. Emphos PS21 is an anionic surfactant which is also adsorbed on the particles but it does not affect the pH.

The stability of the suspensions was evaluated by measuring the viscosity and its variation in time. Rheological measurements were performed using a rotational rheometer (Haake RS50, Germany) with a double-cone and plate measuring system.

## 2.3. Substrates and coatings

Stainless steel 316L plates (8 cm × 4 cm × 2 mm) were used as substrates. Samples were cleaned in an ultrasonic bath, immersed in ethanol and then dipped in the sol and withdrawn at 4 cm min<sup>-1</sup>. After being at room temperature for 30 min, samples were heat treated at 450 °C for 30 min.

Two different types of coatings were applied:

- (a) Single coatings from the suspensions containing the different particles.
- (b) Double coatings consisting on a first coating of the SiO<sub>2</sub> hybrid sol without particles, treated at 450 °C during 30 min, followed by a second coating deposited on the top of the first one, of the particle containing suspensions, followed by the same heat treatment. The thickness was measured with a profilometer (Talystep, Taylor Hobson, UK) on a scratch marked on the film after the deposition. The homogeneity, critical thickness and defects of coatings were observed by optical microscopy (Olympus BX41).

## 2.4. Electrochemical assays

Potentiodynamic polarization curves were measured with a Solartron 1280B Electrochemical Unit. The tests were carried out at 37 °C in simulated body fluid (SBF) at pH 7.35 ± 0.05 after 24 h and 10 days of immersion. A traditional three electrode cell was employed. A platinum wire was used as auxiliary electrode and a saturated calomel electrode (SCE, Radiometer) as the reference electrode. Polarization curves were measured from the corrosion potential ( $E_{\text{CORR}}$ ) up to 1.40 V at a sweeping rate of 0.002 V s<sup>-1</sup>. Linear polarization resistance measurements were registered sweeping ±0.010 V around corrosion potential at 0.002 V s<sup>-1</sup>.

Errors were calculated as standard deviations from the media of three independent experiments of each condition, being around 2–3% in the  $x$ -axis for all the data points.

In vitro tests were performed by soaking the coated samples in simulated body fluid (SBF). The samples were immersed in the solution for various times at a constant temperature of 37 °C, maintaining a constant ratio sample area/fluid volume of 0.35 cm<sup>2</sup>/ml. The presence of apatitic phases (the bone mineral phase) onto the samples surface, was evaluated scanning electronic microscopy (SEM) after in vitro tests.

## 3. Results

### 3.1. Characterization of particles and suspensions

The density, average size and specific surface area of the particles are shown in Table 1. The particle size distributions of the hydroxyapatite and glass particles are 5 ± 1 μm and 39 ± 1 μm, respectively. The glass–ceramic particles present a wider distribution with an average diameter of 16 ± 1 μm.

Table 1  
Mean size, density and specific surface area of the particles

Particles	Surface area ( $\text{g}/\text{m}^2$ )	Average diameter ( $\mu\text{m}$ )	Density ( $\text{g}/\text{cm}^3$ )
Glass	$0.3 \pm 0.1$	$39 \pm 1$	$2.92 \pm 0.1$
Glass-ceramic	$0.8 \pm 0.1$	$16 \pm 1$	$2.99 \pm 0.1$
Hydroxyapatite	$2.4 \pm 0.1$	$5 \pm 1$	$3.11 \pm 0.1$

The rheology of the silica sol and the different suspensions was evaluated as a function of time. The hybrid silica sol had a viscosity of 2.4 mPa s and remains stable for at least two weeks. The addition of TPAH to the glass and glass ceramic containing suspensions raises the viscosity up to 7 mPa s. Both suspensions maintain stable for 8 h, gelling with further ageing. When hydroxyapatite particles are used, the addition of 2 wt% respect to solids of phosphate ester is enough to obtain stable suspensions with initial viscosity of 3 mPa s that increases to 5 mPa s after 5 h being stable for 3 days.

### 3.2. Characterization of the coatings

Crack-free single and double coatings were obtained with homogeneous particle distributions and no observable defects (Fig. 1). The single coatings containing glass

and glass ceramic particles have a critical thickness, defined as the greatest thickness without cracks,  $>1.5 \mu\text{m}$ , and particles with an average of 40 m diameter and  $16 \mu\text{m}$  diameter. On the other hand, hydroxyapatite single coatings had a critical thickness around  $2 \mu\text{m}$  and average particle sizes between 5 and  $8 \mu\text{m}$  diameters. The hybrid  $\text{SiO}_2$  coating applied as inner layer in the double coatings was  $1 \mu\text{m}$  thick.

In vitro tests revealed that all the coatings induced the formation of a semi crystalline hydroxyapatite (HA) rich layer onto the substrate surface as a result of the chemical reaction of the particles with the surrounding body fluid, considered as a preliminary signal of bioactivity after immersion in SBF [15]. After 14 days of immersion in SBF, a spread area of the glass ceramic and hydroxyapatite (HA) containing coatings was covered by an HA film. Besides, glass particle containing coatings had only localized areas with HA film deposited on its surface. Fig. 2(a) shows the glass ceramic containing coating that has induced the formation of a HA deposit on its surface. Fig. 2(b), shows the flaws generated around the bioactive glass particles during the reaction between the particle and the surrounding fluid.

The electrochemical in vitro assays revealed that the presence of the coating improves the corrosion

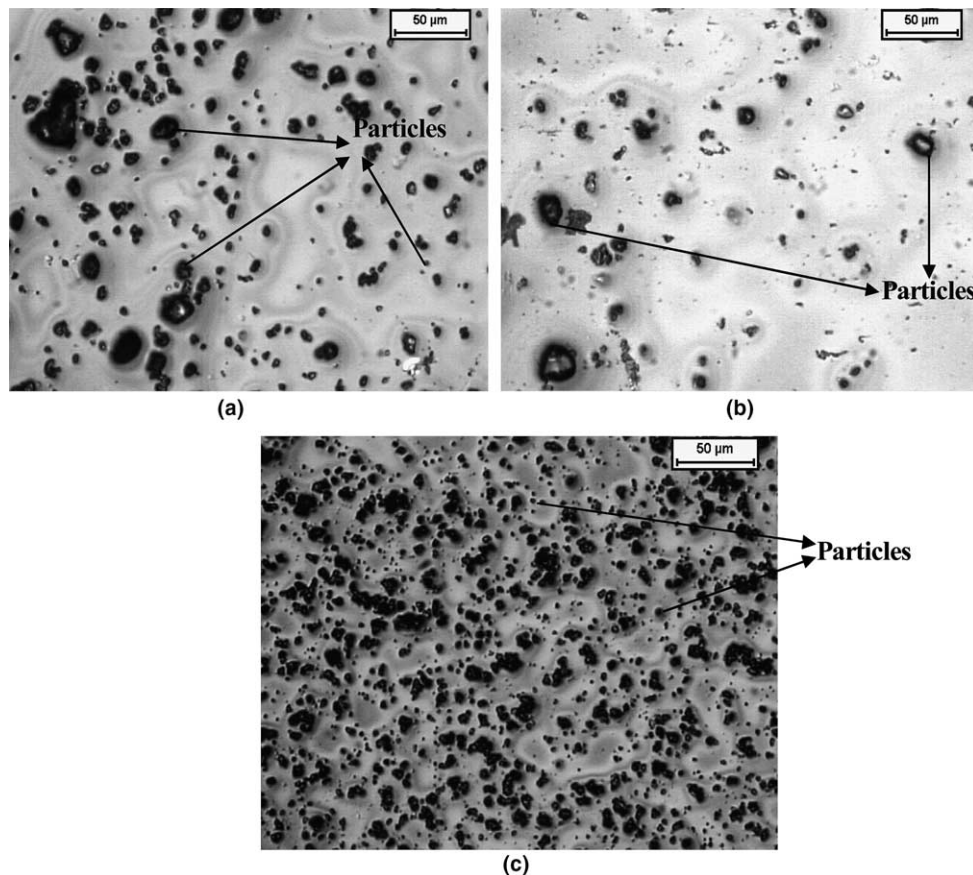


Fig. 1. Reflectance optical microscopy photographs of: (a) glass ceramic, (b) glass and (c) hydroxyapatite containing coatings  $\times 200$ .

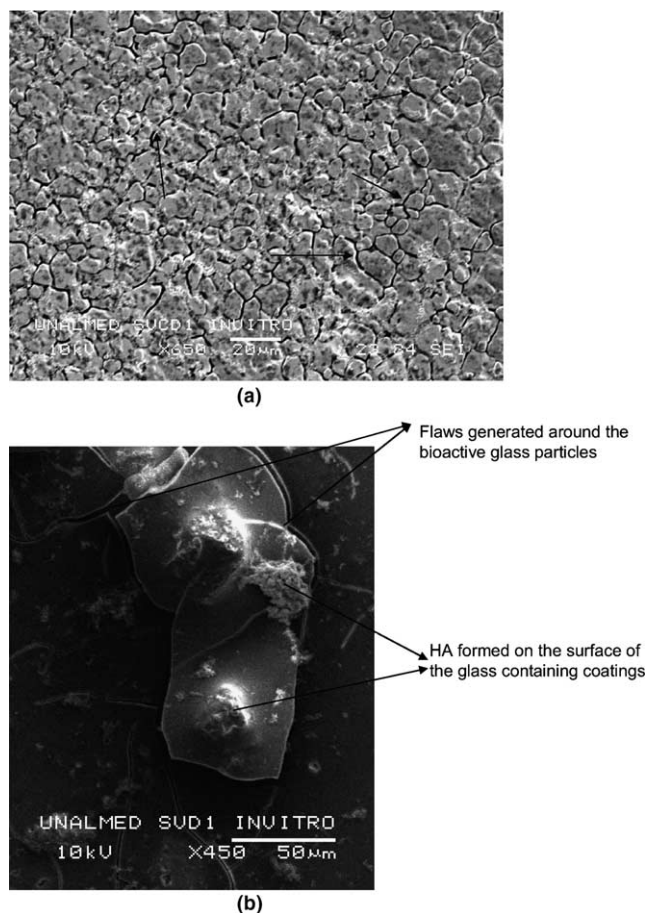


Fig. 2. (a) SEM photomicrograph of the HA deposit formed on a glass ceramic containing coating after 14 days of immersion in SBF. The arrows show some cracks on the apatitic phase formed onto the surface. (b) SEM photomicrograph of a flaw generated around bioactive glass particles under dissolution in SBF.

resistance of the substrate after immersion in SBF, indicating that the coating acts as a barrier to prevent electrolyte from reaching the metal surface.

The single and double coatings have greater corrosion resistant (Fig. 3) than the bare substrate. All the potentiodynamic data corresponding to the three kind of particles show a decrease of the passivation current density ( $i_{\text{pass}}$ ), that is the current density to which the metal remains passive, and a shift to positive potentials of the breakdown potential ( $E_b$ , potential in which passivity breaks and current density increases in a monotonic way with potential) compared to the bare material. Thus, we observed an increase in the passive region from  $-0.31 \pm 0.05$  V to  $-0.4 \pm 0.05$  V for the bare alloy, to  $-0.32 \pm 0.04$  V to  $-0.75 \pm 0.03$  V for the coated samples despite the kind of particle employed. Similar results have been obtained for monolayer coatings containing the three types of particles. Similar results have been obtained for monolayer coatings containing the three types of particles.

After 10 days of immersion in SBF both single and double coating samples containing hydroxyapatite and glass particles, deteriorated and therefore the passive current intensities are bigger than in the initial time. Glass ceramic containing particles applied as double layer, have different passive current than the others after 10 days of immersion (Fig. 4). These samples have smaller current densities than the ones after 24 h of immersion although  $E_b$  shifted cathodic.

Coating porosities that means exposed area to electrolyte, can be estimated according to the equation.

$$P = \frac{R_{ps}}{R_p} \times 10^{-\frac{|\Delta E_{\text{corr}}|}{b_a}} \times 100, \quad (1)$$

where  $R_p$  is the polarization resistance of the coating,  $R_{ps}$  is the polarization resistance of the bare steel,  $b_a$  is the Tafel slope of the bare stainless steel and  $\Delta E_{\text{corr}}$  is the difference in corrosion potential between the coated and bare substrate [13,16,17]. Tafel slope was determined from the data of Fig. 3 and a value of  $0.505 \text{ V dec}^{-1}$  was obtained.  $R_{ps}$  and  $R_p$  and porosities values calculated according Eq. (1) are presented in Table 2.

#### 4. Discussion

The first difference between glass, glass–ceramic and hydroxyapatite suspensions is found in the different type and concentration of dispersant needed to obtain stability. The HA suspension, with particle size centered on  $5 \mu\text{m}$ , is easily stabilized with low concentrations of phosphate ester leading to smaller viscosity and more stable suspensions. On the contrary, the longer content of tetrapropyl ammonium hydroxide (TPAH) used for stabilizing glass and glass–ceramic suspensions are likely due to the big size of the particles, this provoking a viscosity increase. This particle size has been selected for reducing the dissolution rate of the particles on the coatings when soaked in SBF, and studying their effect on the kinetics of HA deposition.

The particle size affects not only the viscosity and stability of the suspensions but the coating thickness. Gallardo et al. [6,7] worked with particles of  $5 \mu\text{m}$  diameter, obtaining coatings up to  $8 \mu\text{m}$  thick. For particles as big as  $39 \mu\text{m}$ , it is difficult to obtain thick coatings because the film around the particles has high probabilities to surpass the critical thickness corresponding to the hybrid composition, generating cracks around it.

In vitro results with coatings with  $40 \mu\text{m}$  particles after 14 days of immersion in SBF show localized deposition of HA whilst for particles about  $5 \mu\text{m}$  the HA deposit completely covered the surface after 7 days of immersion [6,7]. Therefore, the bigger the particles the less reactive for HA deposit forming. After 14 days of immersion in SBF the area covered by HA deposit is

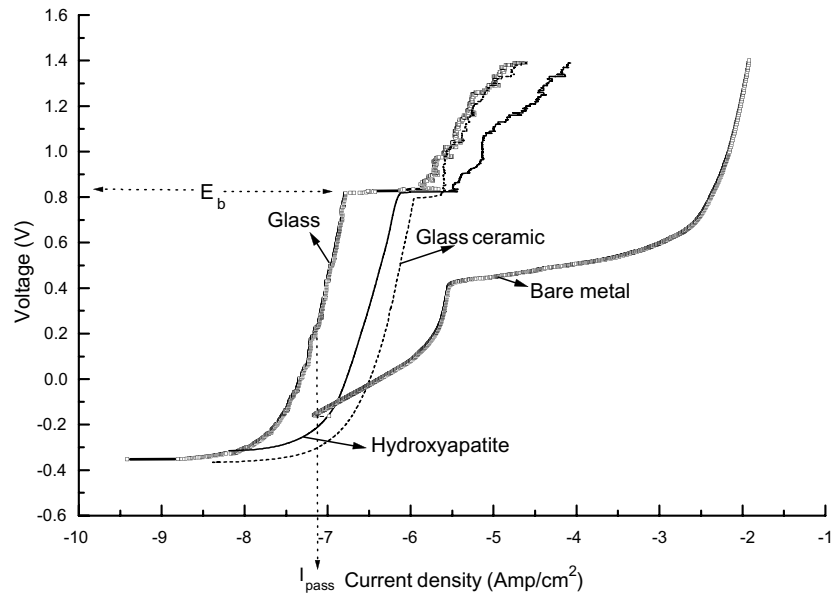


Fig. 3. Anodic polarization curve for double layer coatings containing glass, glass-ceramic and hydroxyapatite, compared with the uncoated substrate after 24h immersion in SBF.

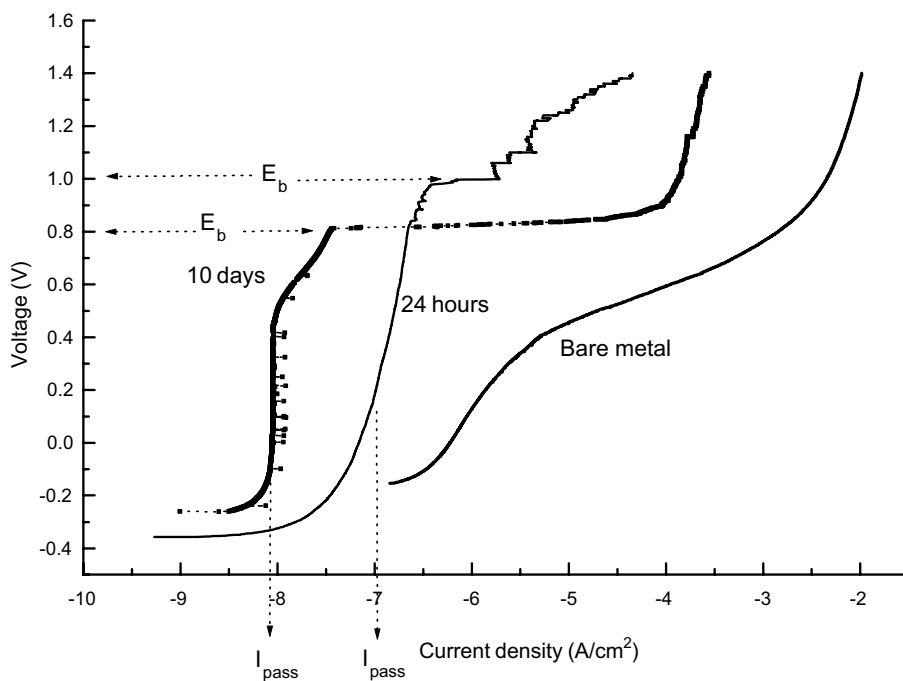


Fig. 4. Anodic polarization curves for a glass-ceramic containing coating applied as double layer, after 24h and 10 days of immersion in SBF.

smaller for the glass containing coatings than for the glass ceramic ones. Therefore the smaller reactivity of glass particles is evident due to their bigger particle size when compared with the glass ceramic particles. Besides, the deposited HA area on glass ceramic and hydroxyapatite containing coating are similar despite the smaller particle size of the hydroxyapatite. This difference is

associated with the smaller reactivity of the hydroxyapatite particles compared with glass ceramic ones.

The mechanism of degradation of mono layer coatings containing bioactive glass particles has been explained through the appearance of flaws, caused by the gradual dissolution of the particles when immersed in SBF, representing a minimum percentage of the total

Table 2  
 $R_{ps}$ ,  $R_p$  and porosity values of all kind of particles in coatings

Kind of particle in coating/immersion time	$E_{corr}/V$	$R_p/M\Omega cm^2$	%P
Bare stainless steel	$-0.201 \pm 0.042$	$0.208 \pm 0.03$	–
<i>Mono layer</i>			
Glass/24h	$-0.273 \pm 0.017$	$2.31 \pm 0.17$	6.60
Glass/10 days	$-0.216 \pm 0.025$	$0.881 \pm 0.09$	22.10
Glass–ceramic/1 h	$-0.288 \pm 0.016$	$1.74 \pm 0.04$	8.17
Glass–ceramic/10 days	$-0.215 \pm 0.024$	$0.820 \pm 0.06$	23.89
HA/24h	$-0.291 \pm 0.001$	$1.06 \pm 0.05$	13.24
HA/10 days	$-0.288 \pm 0.015$	$0.570 \pm 0.07$	24.95
<i>Double layer</i>			
Glass/24h	$-0.337 \pm 0.018$	$2.71 \pm 0.12$	4.22
Glass/10 days	$-0.304 \pm 0.022$	$2.59 \pm 0.09$	5.11
Glass–ceramic/1 h	$-0.366 \pm 0.015$	$2.28 \pm 0.12$	4.42
Glass–ceramic/10 days	$-0.285 \pm 0.013$	$7.11 \pm 0.15$	2.02
HA/24h	$-0.336 \pm 0.021$	$1.91 \pm 0.08$	6.02
HA/10 days	$-0.223 \pm 0.025$	$0.92 \pm 0.07$	20.64

area of the coating. These defects grow as the glass particles dissolve, compromising only restricted zones and promoting the localized corrosion of the metal [7]. This mechanism can be also applied for single coatings for all kind of particles used in this work. Fig. 2(b) illustrates the formation of flaws surrounding glass particles of 25–30  $\mu m$  that permits the entrance of the electrolyte.

Similar to mono layer coatings, the double films improved the corrosion resistance of steel substrate. Additionally to the protector character of the coating containing particles, there is a hybrid  $SiO_2$  coating which has demonstrated electrochemical inhibition of the corrosion and Fe diffusion [7]. In the case of glass ceramic containing coating, the current density of the double layer diminishes in time and porosity seems to be reduced. This effect could be explained through the blockage of pores for the deposition of hydroxyapatite as a result of the reaction between the particles and the solution.

We suggest that the film is acting as barrier to electrolyte diffusion indicating that it is with pores and/or coatings initial defects at the first stages of immersion, in agreement with the microscopic observation of the coating as shown in Fig. 1. The two coatings as well as the hybrid structure of the film reduces porosity in the coating as already demonstrated by other authors [6,14]. After 10 days of immersion, localized corrosion occurring in the flaws created by dissolution of bioactive particles propagates increasing the surface in contact with the electrolyte, except in the glass ceramic double coating where porosity defect density is reduced.

The three kind of particles used in this work are bioactive because they induced the formation of a HA film on the surface of the particles containing coatings after some time of immersion in SBF. This reactivity depends on the particle size; the larger the size, the slower the reactivity of the particles containing coatings.

After 14 days of immersion in SBF, hydroxyapatite and glass ceramic coatings presented a similar area covered by the products of the dissolution of the particles in SBF. Despite the smaller particles size of the hydroxyapatite and therefore its bigger specific surface area the hydroxyapatite particles were less reactive than glass ceramic ones.

Despite properties and size of the particles, the electrochemical data showed that protection of the coatings is evident. As shown by electrochemical measurements, the coating acts as protecting barrier against the electrolyte access to the metal surface. This barrier effect is increased by the first hybrid  $SiO_2$  coating that prevents the contact of electrolyte with the substrate after the dissolution of bioactive particles.

Glass ceramic containing coatings have the best bioactive and protective behavior as indicated by data in Fig. 4. This protection is likely achieved by the blockage of flaws generated by particle dissolution by the deposited apatitic phase.

In vitro electrochemical spectroscopy impedance experiments and in vivo assays on Law rats are already in progress with the aim of gaining a better insight in the behavior of the system.

## 5. Conclusions

It is possible to deposit bioactive particle containing films on stainless steel 316L using dispersants to obtain a good particle suspension.

Single and two-layer coatings improve corrosion resistance of the steel substrate. Corrosion of coatings containing 20  $\mu m$  diameter average and 5  $\mu m$  diameter average particles are comparable. This protection diminishes in time due to the entrance of the electrolyte into pores or small fissures.

After 10 days of immersion in SBF, the glass ceramic double layer coating has better corrosion resistance than after 24h. This likely indicates that the dissolution products are blocking effectively the electrochemical process at the pores and the defects of the coating, acting as a protective layer against corrosion and ion diffusion.

The three kind of particles used in this work show bioactive signals since they induced the formation of a HA film after some time of immersion in SBF. This reactivity depends on the particle size; the larger the size, the slower the reactivity of the particles containing coatings.

## Acknowledgments

The authors thank CYTED project VIII-9 and Network VIII-E, and Colciencias (Colombia) for the financial support of this work.

## References

- [1] K. Meinert, C. Uerpmann, J. Matschullat, G.K. Wolf, Surf. Coat. Technol. 103&104 (1998) 58.
- [2] O. de Sanctis, L. Gómez, N. Pellegrini, A. Marajofsky, C. Parodi, A. Durán, J. Non-Cryst. Solids 121 (1990) 338.
- [3] M. Guglielmi, J. Sol–Gel Sci. Technol. 8 (1997) 443.
- [4] M. Mening, C. Schelle, A. Durán, J.J. Damborenea, M. Guglielmi, G. Brusatin, J. Sol–Gel Sci. Technol. 13 (1998) 717.
- [5] P. Galliano, J.J. de Damborenea, M.J. Pascual, A. Durán, J. Sol–Gel Sci. Technol. 13 (1998) 723.
- [6] J. Gallardo, P. Galliano, R. Moreno, A. Durán, J. Sol–Gel Sci. Technol. 19 (2000) 107.
- [7] J. Gallardo, P. Galliano, A. Durán, J. Sol–Gel Sci. Technol. 21 (2001) 65.
- [8] C. García, R. Moreno, A. Durán, J. Sol–Gel Sci. Technol., in press.
- [9] P.C. Innocenzi, M. Guglielmi, M. Gobbin, P. Colombo, J. Eur. Ceram. Soc. 10 (1992) 431.
- [10] J.J. de Damborenea, J. Gallardo, A. Durán, Corros. Sci. 46 (2004) 795.
- [11] K. Izumi, H. Tanaka, Y. Uchida, N. Toghe, T. Minami, J. Non-Cryst. Solids 147 (1992) 483.
- [12] C. García, C. Paucar, J. Gaviria, A. Durán, Bioceramics, Vol. 17. Proceedings of the 17th International Symposium on Ceramics in Medicine International Society for Ceramics in Medicine (ISCM), New Orleans, USA, 2004 Trans Tech Publications Ltd., in press.
- [13] J. Creus, H. Mazille, H. Idrissi, Surf. Coat. Technol. 130 (2000) 224.
- [14] J. Gallardo, A. Durán, D. di Martino, R. Almeida, J. Non-Cryst. Solids 298 (2002) 219.
- [15] T. Kokubo, H. Kushitani, C. Ohtsuki, S. Sakka, J. Mater. Sci.: Mater. Med. 3 (1992) 79.
- [16] B. Elsener, A. Rota, H. Bohni, Mater. Sci. Forum 44&45 (1989) 28.
- [17] B. Matthes, E. Broszeit, J. Aromaa, Surf. Coat. Technol. 49 (1991) 489.